 cmes, vol.5, no.6, pp.497-514, 2004

Finite Element Modeling of Thin Layers

Dan Givoli[1]

Abstract: Very thin layers with material properties which significantly differ from those of the surrounding medium appear in a variety of applications. Traditionally there are two extreme ways of handling such layers in finite element analysis: either they are fully modelled or they are totally ignored. The former option is often very expensive computationally, while the latter may lead to significant inaccuracies. Here a special technique of modeling thin layers is devised within the framework of the finite element method. This technique constitutes a prudent compromise between the two extremes mentioned above. The layer is replaced by an *interface*, namely a line or a surface (with zero thickness) in two- or three-dimensional analyses, respectively. Special *jump conditions* are imposed on this interface to model the effect of the layer. The method is presented in various configurations and variants, and its performance in one representative two-dimensional case is demonstrated via numerical experiments.

keyword: Thin layer, Thin Film, Finite Element, Interface, Coating.

1 Introduction

Very thin layers with distinct material properties frequently appear in Finite Element (FE) computations. Examples include exterior coating of structures, glue between two parts of a structure, the "mushy zone" between a liquid phase and a solid phase in contact, thin films on substrates in electromagnetic devices, and coating of fibers in composite materials. See, e.g., [Achenbach and Zhu (1989), Achenbach and Zhu (1990), Masters and Salamon (1994), Cai and Bangert (1996), Sham and Tichy (1997), Boutry, Bosseboeuf, Grandchamp and Coffignal (1997), Body, Reyne and Meunier (1997), Sung, Choi and Yoo (1999), Zhang, Bower, Xia and Shih (1999), Yue, Eggeler and Stockhert (2001), Hoppe and Nash (2002), Suess, Tsiantos, Schrefl, Scholz and Fidler (2002), Genna, Paganelli, Salgarello and Sapelli (2003), Subramaniam and Ramakrishnan (2003)] for recent applications. In such cases the thickness of the layer is at least an order of magnitude smaller than the global dimensions of the structure, and often two or three orders of magnitude smaller. The layer may have a structural role (as in the case of glue), a thermal role (as in the case of a thin thermal insulator), an electromagnetic or optical role, etc., depending on the application. Methods other than FE have also been used for the analysis of thin layers [Zhang and Yao (2002), Chen and Liu (2001)].

Traditionally there are two extreme ways of handling very thin layers in FE computations. One option is simply to totally ignore the layer, under the assumption that its effect on the solution of the problem at hand is negligible. This assumption may sometimes be inappropriate, especially if the material properties of the layer deviate significantly from those of the media around it. At the other extreme, the layer can be fully included in the FE model. In this case, the mesh inside the layer must be sufficiently fine to resolve the solution there. More importantly, one needs to keep the element aspect-ratio close to one for well-conditioning purposes, implying that the mesh must be fine in the direction *parallel* to the layer, not only normal to it. It is well known that needle-like elements may lead to severe ill-conditioning. In addition, one needs to coarsen the mesh *gradually* away from the layer, which means that the mesh must be fine in a much larger region than the layer itself.

In this paper we propose a method of modeling thin layers in FE computations, which constitutes a compromise between the two extremes mentioned above. The layer is modelled here as an *interface*, namely a line or a surface (with zero thickness) in two- or three-dimensional analyses, respectively. The effect of the layer on the solution is modeled by means of *jump conditions* across this interface, which are incorporated into the FE formulation. In-

[1] Department of Aerospace Engineering and Asher Center for Space Research Technion — Israel Institute of Technology Haifa 32000, Israel
E-mail: givolid@aerodyne.technion.ac.il
Tel.: +972-4-8292308, Fax: +972-4-8293193

dependent degrees of freedom are defined on both sides of the interface. In this way, the layer is taken into account in the computation, but it does not occupy a region in the geometrical model and no special mesh refinement is needed. The method is thus only slightly less efficient than the procedure of ignoring the layer altogether but is significantly more accurate. On the other hand, it is more efficient than the method of modeling by FEs the entire region of the layer. The setup is illustrated in Fig. 1.

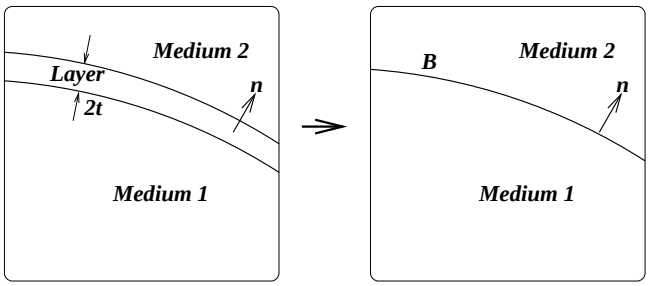

Figure 1 : Replacing a thin layer by an interface.

The idea to replace a layer by an interface is borrowed from a recent work by Hashin [Hashin (2001), Hashin (2002)]. Hashin considered a thin layer (an "interphase") which separates two phases; each of the three phases may have its own material properties. The layer is then replaced by an interface, and jump conditions are derived on it which approximately replace the original continuity conditions that have to be satisfied on both sides of the layer. In [Hashin (2001)] this was done for conductivity problems governed by Laplace's equation in each phase. In [Hashin (2002)] the same procedure, although much more complicated technically, was applied to linear elasticity. Hashin's jump conditions were proposed as a tool for deriving approximate *analytic* solutions to problems involving embedded thin layers, such as the problem of determining the effective properties of composites with coated inclusions. Unfortunately Hashin's conditions are not convenient for FE computation; their form is incompatible with the standard variational form of the problem, and thus they are not easily incorporated into a FE formulation.

Here we develop other interface conditions which are highly compatible with the standard FE formulation. We derive two types of such interface conditions: exact nonlocal conditions, and approximate local conditions. The derivation of the former shows that it is sometimes possible to replace the layered problem with an *exactly equivalent* interface problem. The exact nonlocal conditions may also serve as a starting point for deriving the approximate local conditions in a systematic manner. However, they are not very practical for actual computation; the nonlocality carries with it a computational burden that does not always justify the replacement of the layer with an interface. On the other hand, the local conditions proposed here are practical and useful.

Following is the outline of the rest of the paper. In Section 2 we start with a simple one-dimensional configuration, and show how a layer can be replaced by an interface in an *exact* manner. This development bears theoretical interest but is associated with some clear deficiencies. Therefore in Section 3 we *approximate* the representation of the layer, still in one dimension. In Section 4 we consider a two-dimensional scalar (e.g., heat conduction) problem. Again we show how a layer can be replaced by an interface *exactly*. As in the one-dimensional case, this technique is of theoretical interest but is not practical in the general case. In Section 5, we consider an alternative *approximate* modeling procedure. We discuss both low-order and higher-order schemes. In Section 6 we show how the scheme can be extended in various ways. In particular we discuss the elastic case. Numerical experiments for the representative case of conductivity in two dimensions are presented in Section 7. We conclude in Section 8 with some remarks.

2 The 1D-Layer Formulation: Exact Treatment

We consider a *one-dimensional (1D)* problem in the interval $r_1 \le r \le r_2$, where $r_1 < 0$ and $r_2 > 0$. This interval may represent for example a 1D rod or the radial direction in an annular domain under axi-symmetric conditions. The interval $\Omega \equiv (r_1, r_2)$ is divided into three subintervals: $\Omega_1 \equiv (r_1, -t)$, $\Omega_L \equiv (-t, t)$ (the layer, with thickness $2t$) and $\Omega_2 \equiv (t, r_2)$. A second-order differential equation governs in each of the regions Ω_j ($j = 1, L, 2$). To fix ideas we consider the equation

$$L_j u_j \equiv -\kappa_j u_j'' + s_j u_j = 0 \tag{1}$$

(no sum over j) where κ_j is constant and s_j is a nonnegative function. We take the external boundary conditions

$$u_1(r_1) = 0 \qquad , \qquad \kappa_2 u_2'(r_2) = f \ , \tag{2}$$

where f is a given number. On the two ends of the layer we have the continuity conditions

$$u_1(-t) = u_L(-t) \quad , \quad u_L(t) = u_2(t) \; , \tag{3}$$

$$\kappa_1 u_1'(-t) = \kappa_L u_L'(-t) \quad , \quad \kappa_L u_L'(t) = \kappa_2 u_2'(t) \; . \tag{4}$$

The conditions in (3) enforce the continuity of the primary variable u (e.g., temperature), whereas the conditions in (4) require the continuity of the 'flux' $\kappa u'$.

In the layer we solve the problem analytically. Suppose the general solution in the layer is of the form

$$u_L(r) = A\,F(r) + B\,G(r). \tag{5}$$

Here F and G are known functions, and A and B are unknown constants. From (5) we can write

$$\begin{bmatrix} F(-t) & G(-t) \\ F(t) & G(t) \end{bmatrix} \begin{Bmatrix} A \\ B \end{Bmatrix} = \begin{Bmatrix} u_L(-t) \\ u_L(t) \end{Bmatrix}. \tag{6}$$

By solving this set of equations we express A and B in terms of $u_L(-t)$ and $u_L(t)$. Then we have:

$$\begin{aligned} \kappa_L u_L'(-t) &= \kappa_L (AF'(-t) + BG'(-t)) \\ &\equiv \alpha u_1(-t) + \beta u_2(t) \; , \end{aligned} \tag{7}$$

$$\begin{aligned} \kappa_L u_L'(t) &= \kappa_L (AF'(t) + BG'(t)) \\ &\equiv \gamma u_1(-t) + \delta u_2(t) \; . \end{aligned} \tag{8}$$

We have replaced the subscript L on the right side of (7) and (8) owing to the condition (3). In (7) and (8), α, β, γ and δ are constants given by

$$\begin{aligned} \alpha &= \frac{\kappa_L}{D} \left[G(t)F'(-t) - G'(-t)F(t) \right] \; , \\ \beta &= \frac{\kappa_L}{D} \left[G'(-t)F(-t) - G(-t)F'(-t) \right] \; , \end{aligned} \tag{9}$$

$$\begin{aligned} \gamma &= \frac{\kappa_L}{D} \left[G(t)F'(t) - G'(t)F(t) \right] \; , \\ \delta &= \frac{\kappa_L}{D} \left[G'(t)F(-t) - G(-t)F'(t) \right] \; , \end{aligned} \tag{10}$$

where

$$D = G(t)F(-t) - G(-t)F(t) \; . \tag{11}$$

From (4), (7) and (8) we finally obtain

$$\begin{aligned} \kappa_1 u_1'(-t) &= \alpha u_1(-t) + \beta u_2(t) \; , \\ \kappa_2 u_2'(t) &= \gamma u_1(-t) + \delta u_2(t) \; . \end{aligned} \tag{12}$$

These two conditions are equivalent to the original conditions (3) and (4).

We remark that the boundary conditions (12) have the form of *Dirichlet-to-Neumann (DtN) boundary conditions*. See the recent reviews [Givoli (1999a), Givoli (1999b)] on the subject. DtN conditions have been incorporated in a FE formulation in order to eliminate an infinite domain [Keller and Givoli (1989)], a singular domain [Givoli, Rivkin and Keller (1992)], or a substructure [Barbone, Givoli and Patlashenko (2003)] from computational domains, to mention the most important applications. Here the DtN condition is used to eliminate a thin layer from the computation.

Now we derive the weak form of the problem consisting of (1), (2) and (12). In Ω_1 we obtain the weak equation for $u \in S_1 \equiv H^1(\Omega_1)$,

$$a_1(w,u) - \alpha w(-t)u(-t) - \beta w(-t)u(t) = 0 \; , \tag{13}$$

for any $w \in S_1$. In Ω_2 we obtain the equation for $u \in S_2 \equiv H^1(\Omega_2)$,

$$a_2(w,u) + \gamma w(t)u(-t) + \delta w(t)u(t) = w(r_2)\,f \; , \tag{14}$$

for any $w \in S_2$. In (13) and (14),

$$a_j(w,u) = \int_{\Omega_j} (w' \kappa_j u' + w s_j u)\, d\Omega \; . \tag{15}$$

To obtain a symmetric formulation, we multiply (13) by $(-\gamma)$ and (14) by β and add the two equations to obtain

$$a(w,u) + b(w,u) + c(w,u) = w(r_2)\beta f \; . \tag{16}$$

Here

$$a(w,u) = -\gamma a_1(w,u) + \beta a_2(w,u) \; , \tag{17}$$

$$b(w,u) = \alpha\gamma w(-t)u(-t) + \beta\delta w(t)u(t) \; , \tag{18}$$

$$c(w,u) = \beta\gamma \left(w(-t)u(t) + w(t)u(-t) \right) . \tag{19}$$

This leads to the symmetric FE matrix problem

$$\boldsymbol{K}\boldsymbol{d} = \boldsymbol{F} \; , \tag{20}$$

where

$$K_{AB} = a(\phi_A, \phi_B) + b(\phi_A, \phi_B) + c(\phi_A, \phi_B) \ , \tag{21}$$

$$F_A = \phi_A(r_2)\beta f \ . \tag{22}$$

Here ϕ_A is the shape function associated with node A. Of course, in practice the FE array construction is implemented on the element level.

The above amounts to the exact elimination of the layer. If the layer is sufficiently thin, we can neglect the thickness of the layer in the geometrical sense. Namely we replace the layer with a single *interface* in the middle of the layer, i.e., at $r = 0$, and allow the discontinuity of u and w across it. Consequently we have two values of u at r=0: $u^-(0)$ and $u^+(0)$. The same applies to w at $r = 0$. Thus, we approximate

$$\begin{aligned} &u(-t) \simeq u^-(0) \ , \ u(t) \simeq u^+(0) \ , \\ &w(-t) \simeq w^-(0) \ , \ w(t) \simeq w^+(0) \ . \end{aligned} \tag{23}$$

With this approximation the boundary conditions (12) become the jump conditions

$$\begin{aligned} \kappa_1(u^-)'(0) &= \alpha u^-(0) + \beta u^+(0) \ , \\ \kappa_2(u^+)'(0) &= \gamma u^-(0) + \delta u^+(0) \ , \end{aligned} \tag{24}$$

and the bilinear forms (17)–(19) are replaced by

$$a(w,u) = -\gamma \hat{a}_1(w,u) + \beta \hat{a}_2(w,u) \ , \tag{25}$$

$$b(w,u) = \alpha\gamma w^-(0)u^-(0) + \beta\delta w^+(0)u^+(0) \ , \tag{26}$$

$$c(w,u) = \beta\gamma \left(w^-(0)u^+(0) + w^+(0)u^-(0)\right) . \tag{27}$$

Here

$$\begin{aligned} \hat{a}_1(w,u) &= \int_{\hat{\Omega}_1} (w'\kappa_1 u' + w s_1 u)\, d\Omega \ , \\ \hat{a}_2(w,u) &= \int_{\hat{\Omega}_2} (w'\kappa_2 u' + w s_2 u)\, d\Omega \ . \end{aligned} \tag{28}$$

The "extended domains" $\hat{\Omega}_1$ and $\hat{\Omega}_2$ are defined by

$$\hat{\Omega}_1 = \Omega_1 \cup (-t, 0) \qquad , \qquad \hat{\Omega}_2 = \Omega_2 \cup (0, t) \ , \tag{29}$$

namely each subdomain includes half of the layer. The FE matrix formulation remains (20)–(22), with these new definitions.

3 The 1D-Layer Formulation: Approximation

The formulation above suffers from two deficiencies:

1. It requires the knowledge of the exact solution in the layer, namely the functions F and G in (5), since the coefficients α, β, γ and δ depend on them. These functions are not always easy to obtain in the general case.

2. The analogous treatment in the *multi-dimensional* case results in interface conditions which are *nonlocal*, as we shall see later. Such nonlocal conditions are relatively hard to work with computationally, and may render the whole construction nonpractical. (In 1D the "interface" is a single point and so the issue of non-locality does not arise.)

Therefore, we shall consider now an approximation for the interface conditions derived in the previous section, which will become especially useful when we consider the multi-dimensional case.

We assume that the solution inside the layer has the form (5). However, rather than considering F and G to be the exact elementary solutions of the differential equation (1), we take F and G to be the *linear* functions:

$$F(r) = \frac{1}{2}\left(1 - \frac{r}{t}\right) \qquad , \qquad G(r) = \frac{1}{2}\left(1 + \frac{r}{t}\right) \ . \tag{30}$$

Note that these are in fact the FE shape functions of a 1D linear element. With these functions the linear combination on the right side of (5) can represent *any* linear function in the layer. The approximation in the layer given by (5) and (30) is justified since the layer is thin by assumption and every smooth function can be locally approximated by a linear function. Another way to justify (30) is to write the solution in the layer as a Taylor expansion up to the linear term. This approximation is expected to be excellent unless the exact solution inside the layer changes sharply.

With F and G given by (30) the matrix appearing in (6) becomes the identity, and thus we obtain from (6)

$$A = u_L(-t) \qquad , \qquad B = u_L(t) \ . \tag{31}$$

Then (9)–(11) reduce to $D = 1$ and

$$\alpha = \gamma = -\kappa_L/(2t) \qquad , \qquad \beta = \delta = \kappa_L/(2t) \ . \tag{32}$$

Hence the boundary conditions (12) become

$$\kappa_1 u_1'(-t) = \frac{\kappa_L}{2t}\,(u(t)-u(-t)) \equiv \frac{\kappa_L}{2t}[u]\ , \tag{33}$$

$$\kappa_2 u_2'(t) = \frac{\kappa_L}{2t}\,(u(t)-u(-t)) \equiv \frac{\kappa_L}{2t}[u]\ . \tag{34}$$

Here

$$[u] \equiv u(t)-u(-t) \tag{35}$$

is the *jump* of u across the layer. Thus, the boundary conditions become simple jump conditions. We also note that the two approximate jump conditions (33) and (34) on the two sides of the layer turn out to have the same right hand side. Thus, we can replace either (33) or (34) by the flux continuity condition

$$\kappa_1 u_1'(-t) = \kappa_2 u_2'(t)\ . \tag{36}$$

The physical meaning of the conditions (33)–(36) is clear. Since $[u]/(2t)$ is an approximation of du/dr in the layer, then $(\kappa_L/(2t))[u]$ approximates the flux in the layer. Thus conditions (33)–(36) dictate that the flux across the layer remains constant.

If the layer is very thin we can represent it by a single interface. In this case the boundary conditions (33) and (34) become the interface jump conditions

$$\kappa_1 (u^-)'(0) = \frac{\kappa_L}{2t}[u]\ , \tag{37}$$

$$\kappa_2 (u^+)'(0) = \frac{\kappa_L}{2t}[u]\ , \tag{38}$$

where $[u]$ is the *jump across the interface*,

$$[u] \equiv u^+(0)-u^-(0)\ . \tag{39}$$

The weak and FE formulations given in the previous section remain the same; simply the expressions (32) are used for the coefficients α, β, γ and δ appearing in the definitions of the bilinear forms (17)–(19) and (25)–(27). After dividing throughout by the common factor $\kappa_L/(2t)$, and denoting $b^*(w,u) = b(w,u)+c(w,u)$ we get the weak equation

$$a(w,u)+b^*(w,u) = w(r_2)\,f\ , \tag{40}$$

where

$$a(w,u) = \hat{a}_1(w,u)+\hat{a}_2(w,u)\ , \tag{41}$$

$$b^*(w,u) = \frac{\kappa_L}{2t}(w^+(0)-w^-(0))(u^+(0)-u^-(0))$$
$$\equiv \frac{\kappa_L}{2t}[w][u]\ . \tag{42}$$

The product $[w][u]$ is the product of the jump of w and of u across the interface. This leads to the symmetric FE matrix problem $\boldsymbol{Kd} = \boldsymbol{F}$ where

$$K_{AB} = a(\phi_A,\phi_B)+b^*(\phi_A,\phi_B)\ , \tag{43}$$

$$F_A = \phi_A(r_2)\,f\ . \tag{44}$$

It is easy to check that the stiffness matrix $\boldsymbol{K}$ is not only symmetric but also *positive definite*. However, we defer the discussion on this issue to Section 5, where we consider the multi-dimensional case.

4 The 2D-Layer Formulation: An Exact Treatment

Now we consider the *two-dimensional (2D)* case, where the interface replacing the layer is represented by a curve in the plane. In this case an exact treatment of the layer analogous to the one applied in Section 2 leads to *nonlocal* interface conditions. To see this, we consider the case of an annular layer, namely a layer bounded by two concentric circles with radii R_1 and R_2. Thus, the thickness of the layer is $2t = R_2 - R_1$ (see Fig. 1). We use a polar coordinate system (r,θ) whose origin is in the center of the two circles. The region occupied by the layer, denoted Ω_L, separates between two regions, Ω_1 and Ω_2. In each of the Ω_j ($j = 1, L, 2$), a second-order elliptic partial differential equation governs, say,

$$L_j u_j \equiv -\kappa_j \nabla^2 u_j + s_j u_j = f_j \tag{45}$$

(no sum on j) where κ_j is constant and s_j is a nonnegative function. The source f_j may be a general function in Ω_1 and Ω_2 but is assumed to be zero in the layer, i.e., $f_L \equiv 0$. Some boundary conditions are given along the external boundary Γ; for simplicity we take

$$u = 0 \quad \text{on} \quad \Gamma\ . \tag{46}$$

The continuity conditions given on the two sides of the layer are

$$u_1(R_1,\theta) = u_L(R_1,\theta)\ , \quad u_L(R_2,\theta) = u_2(R_2,\theta)\ , \tag{47}$$

$$\kappa_1 u_{1,n}(R_1,\theta) = \kappa_L u_{L,n}(R_1,\theta)\ ,$$
$$\kappa_L u_{L,n}(R_2,\theta) = \kappa_2 u_{2,n}(R_2,\theta)\ . \tag{48}$$

Here $u_{j,n}$ means the normal derivative of u_j. See Fig. 1 for the definition of the normal direction n. In the present case $\partial/\partial n = \partial/\partial r$.

The problem just described may represent various physical situations. One major example is that of linear heat conduction. In this case the κ_j are the thermal conductivities of the different phases.

We start as in Section 2 by considering the exact solution inside the layer. Suppose the radial eigenfunctions are $F_n(r)$ and $G_n(r)$ and the angular functions are $T_n^c(\theta)$ and $T_n^s(\theta)$. Typically $T_n^c = \cos(n\theta)$ and $T_n^s = \sin(n\theta)$. The angular functions are orthogonal in $[0, 2\pi]$, and yield (no sum on n)

$$< T_m^c, T_n^c >= \delta_{mn}/b_n \ , \ < T_m^s, T_n^s >= \delta_{mn}/b_n \ ,$$
$$< T_m^c, T_n^s >= 0 \ . \tag{49}$$

Here δ_{mn} is the Kronecker delta, b_n is an integration factor ($b_n = 1$ if the angular functions are normalized to be orthonormal) and

$$< T_m, T_n > \equiv \int_0^{2\pi} T_m T_n \, d\theta \ . \tag{50}$$

In the layer we have the expansion

$$u_L(r,\theta) = \sum_{m=0}^{\infty} \left(F_m(r) \left(A_m T_m^c(\theta) + B_m T_m^s(\theta) \right) \right.$$
$$\left. + \, G_m(r) \left(C_m T_m^c(\theta) + D_m T_m^s(\theta) \right) \right) \ . \tag{51}$$

Now we substitute $r = R_1$ in (51), apply the functional $< T_m^c, \cdot >$ to both sides of the equation, and use the orthogonality (49). Then we repeat this calculation with $r = R_2$ instead of $r = R_1$ and with T_m^s instead of T_m^c. This yields the matrix relations

$$\begin{bmatrix} F_m(R_1) & G_m(R_1) \\ F_m(R_2) & G_m(R_2) \end{bmatrix} \begin{Bmatrix} A_m \\ C_m \end{Bmatrix} = \frac{1}{b_m} \begin{Bmatrix} < u_L(R_1), T_m^c > \\ < u_L(R_2), T_m^c > \end{Bmatrix}, \tag{52}$$

$$\begin{bmatrix} F_m(R_1) & G_m(R_1) \\ F_m(R_2) & G_m(R_2) \end{bmatrix} \begin{Bmatrix} B_m \\ D_m \end{Bmatrix} = \frac{1}{b_m} \begin{Bmatrix} < u_L(R_1), T_m^s > \\ < u_L(R_2), T_m^s > \end{Bmatrix}, \tag{53}$$

By solving these two systems of equations we express A_m, B_m, C_m and D_m in terms of $u_L(R_1,\theta)$ and $u_L(R_2,\theta)$.

The exact solution (51) also gives

$$u_{L,n}(r,\theta) = \sum_{m=0}^{\infty} \left(F_m'(r) \left(A_m T_m^c(\theta) + B_m T_m^s(\theta) \right) \right.$$
$$\left. + \, G_m'(r) \left(C_m T_m^c(\theta) + D_m T_m^s(\theta) \right) \right) \ . \tag{54}$$

Using (52), (53) and (54), we get from the original continuity conditions (47) and (48) the following boundary conditions:

$$\kappa_1 u_{1,n}(R_1,\theta) = \kappa_L \left(M_{11} u(R_1,\theta) + M_{12} u(R_2,\theta) \right) \ , \tag{55}$$

$$\kappa_2 u_{2,n}(R_2,\theta) = \kappa_L \left(M_{21} u(R_1,\theta) + M_{22} u(R_2,\theta) \right) \ . \tag{56}$$

Here the M_{ij} are integral operators (DtN maps; see [Givoli (1999a), Givoli (1999b)]) that can be derived from the equations above. Their action on a function $u(\theta)$ can be found to be of the form

$$M_{ij} u(\theta) = \sum_{m=0}^{\infty} \alpha_{ijm} < T_m^c(\theta) T_m^c(\cdot) + T_m^s(\theta) T_m^s(\cdot), u(\cdot) > \ , \tag{57}$$

where the α_{ijm} are constants that can be deduced from (52)–(54).

The FE formulation incorporating the boundary conditions (55) and (56) is *nonlocal*; it involves the bilinear forms

$$b_{ij}(w,u) \equiv \kappa_L \int_B w M_{ij} u \, dB \ . \tag{58}$$

Here B is one of the boundaries $r = R_1$ or $r = R_2$. In fact, we can take advantage of the thinness of the layer and take B to be a single interface located on the middle curve of the layer, as we have done in the 1D case and as shown in Fig. 1.

5 The 2D Layer Formulation: Approximation

We shall consider here the 2D case, although the same methodology applies in 3D.

As was already implied in the 1D case, the *exact* replacement of the layer with an interface suffers from two serious deficiencies:

1. It requires the knowledge of the exact solution in the layer, which depends on the geometry of the layer. In the previous section we considered the example of an annular layer; obviously we would rarely have

such a simple geometry. In the general case it may be hard or even impossible to obtain the exact solution in the layer analytically.

2. The interface condition and hence the FE formulation is *nonlocal*. In other situations, like the solution of a problem with an infinite domain, the nonlocality may definitely be something that one is willing to accept to ensure very accurate results; see [Givoli (1999a), Givoli (1999b)]. However, in the case of a thin layer, we should bear in mind that the straightforward (although inefficient) option to simply include the whole layer in the FE model always exists. Thus, the replacement of the layer with an interface would be justified only if this replacement is sufficiently simple and computationally inexpensive. Under these circumstances, it seems that the use of nonlocal interface conditions is generally unjustified in this context.

In this light, we wish to obtain simple approximate interface conditions for the multi-dimensional problem. With this goal in mind, we first pose a few requirements that these conditions have to satisfy:

1. They should be compatible with the standard C^0 FE formulation.
2. They should be local.
3. They should not depend on the geometry of the layer.
4. They should not ruin the symmetry and positivity of the FE stiffness matrix $\boldsymbol{K}$ if $\boldsymbol{K}$ has these properties in the standard formulation.
5. They should not introduce new degrees of freedom (DOF) on the interface in addition to the double u-DOF (one on each side of the interface).

Requirements 1, 2, 4 and 5 together imply (among other things) that the interface conditions on B should have the general form

$$\kappa_1 u^-_{,n} = \alpha^- u^- + \beta^- u^+ + \gamma^- u^-_{,ss} + \delta^- u^+_{,ss} \,, \tag{59}$$

$$\kappa_2 u^+_{,n} = \alpha^+ u^- + \beta^+ u^+ + \gamma^+ u^-_{,ss} + \delta^+ u^+_{,ss} \,. \tag{60}$$

Here s is the direction tangent to the interface, and $u_{,ss}$ is the second tangential derivative. Note that the *first* tangential derivative does not appear in this form since it would lead to non-symmetric terms in the FE formulation. One way to obtain conditions of the form (59) and (60) is to first obtain nonlocal exact conditions and then to localize them, as in [Givoli and Patlashenko (2002)]; however, this procedure is geometry dependent and thus would violate requirement 3 above. Hence we will use direct ways to derive interface conditions of the form (59) and (60).

Locally in the layer we use an orthogonal coordinate system (r,s), as shown in Fig. 2. The layer is bounded by the curves $r=-t$ and $r=t$. The interface B that replaces the layer is the middle curve $r=0$.

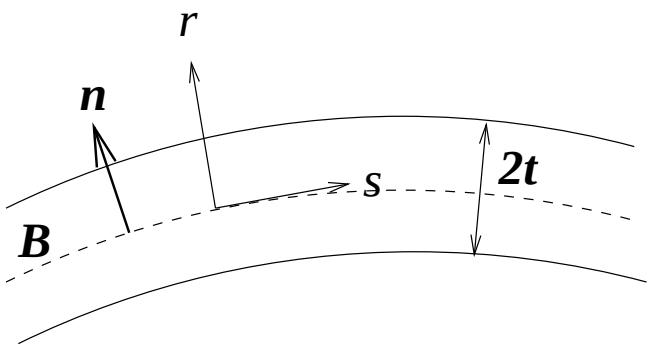

Figure 2 : A layer in a two-dimensional configuration.

5.1 Interface Conditions Involving Only Function Values

In the simplest interface conditions that have the form (59) and (60), $\gamma^- = \gamma^+ = \delta^- = \delta^+ = 0$, namely no s-derivatives appear but only function values. Such a condition is obtained if we assume that the solution in the layer, u_L, depends only on r and not on s. Momentarily we shall relate to the validity of this simplification. In this case we can write u_L as in (5), with $F(r)$ and $G(r)$ given by (30), as we did in 1D. Following the 1D calculation, this immediately leads to boundary conditions of the form (33) and (34), or, if the layer is replaced by an interface, to interface conditions on B of the form (37) and (38), i.e.,

$$\kappa_1 u^-_{,n} = \frac{\kappa_L}{2t}[u] \,, \tag{61}$$

$$\kappa_2 u^+_{,n} = \frac{\kappa_L}{2t}[u] \,, \tag{62}$$

where $[u] \equiv u^+(0,s) - u^-(0,s)$.

The physical interpretation of these conditions is as follows. Since the quantities appearing on either side of (61) and (62) are normal fluxes, these equations imply that the normal flux remains constant across the layer or interface. In other words, flux loss due to "flow" in the tangential direction s is ignored. One can argue that if the layer is very thin it makes sense to ignore the tangential flux in the interface conditions. To see this, assume that the thickness of the layer is vanishingly small, so that it is indeed an interface rather than a layer. Then a tangential flux can only mean the flux "flowing" along the interface, which has no effect over the coupling between the two media on both sides of the interface. Only the normal flux is responsible to the passage of "information" from one medium to another across the interface. Thus the tangential component of the flux is not relevant in the interface condition. If the layer has a finite thickness the tangential flux does have some effect on the coupling between the two media, but arguably a small one.

Now we derive the weak form of the problem. In $\hat{\Omega}_1$ (see (29) for the definition) we obtain the weak equation (for any w in the weighting space)

$$a_1(w,u) - \frac{\kappa_L}{2t}\int_B w_1(u_2-u_1)\,dB = (w,f)_1 \,. \tag{63}$$

In $\hat{\Omega}_2$ we obtain the equation

$$a_2(w,u) + \frac{\kappa_L}{2t}\int_B w_2(u_2-u_1)\,dB = (w,f)_2 \,. \tag{64}$$

Here

$$a_j(w,u) = \int_{\hat{\Omega}_j} (\nabla w\cdot\kappa_j\nabla u + w s_j u)\,d\Omega \,, \tag{65}$$

$$(w,f)_j = \int_{\hat{\Omega}_j} w f\,d\Omega \,. \tag{66}$$

The different signs of the interface B terms in (63) and (64) originate from the fact that the normal n is pointing out of $\hat{\Omega}_1$ but *into* $\hat{\Omega}_2$ (see Fig. 1). By adding the two weak equations we obtain the single equation

$$a(w,u) + b(w,u) = (w,f) \,. \tag{67}$$

Here

$$a(w,u) = a_1(w,u) + a_2(w,u) \,, \tag{68}$$

$$\begin{aligned} b(w,u) &= \frac{\kappa_L}{2t}\int_B (w_2-w_1)(u_2-u_1)\,dB \\ &\equiv \frac{\kappa_L}{2t}\int_B (w^+-w^-)(u^+-u^-)\,dB \\ &\equiv \frac{\kappa_L}{2t}\int_B [w][u]\,dB \,, \end{aligned} \tag{69}$$

$$(w,f) = (w,f)_1 + (w,f)_2 \,. \tag{70}$$

This leads to the symmetric FE matrix problem $\mathbb{K}\boldsymbol{d} = \boldsymbol{F}$ where

$$\boldsymbol{K} = \boldsymbol{K}^a + \boldsymbol{K}^b \,, \tag{71}$$

$$K^a_{AB} = a(\phi_A,\phi_B) \,, \tag{72}$$

$$K^b_{AB} = b(\phi_A,\phi_B) \,, \tag{73}$$

$$F_A = (\phi_A, f) \,. \tag{74}$$

Here the ϕ_A are the shape functions.

It is easy to show that the interface stiffness matrix $\mathbb{K}^b$ is not only symmetric but also positive semi-definite. The following calculation proves this:

$$\begin{aligned} \boldsymbol{v}^T\boldsymbol{K}^b\boldsymbol{v} &= \sum_{A,B} v_A K^b_{AB} v_B = \sum_{A,B} v_A b(\phi_A,\phi_B) v_B \\ &= b\left(\sum_A v_A\phi_A, \sum_B v_B\phi_B\right) \end{aligned} \tag{75}$$

$$= b(v^h,v^h) = \frac{\kappa_L}{2t}\int_B (v^h_2 - v^h_1)^2\,dB \geq 0 \,. \tag{76}$$

Since $\boldsymbol{K}^b$ is positive semi-definite, and since $\boldsymbol{K}^a$ (the standard stiffness matrix) is known to be positive definite, their sum, which is the total stiffness matrix $\mathbb{K}$, is positive definite. This shows that requirement 4 above is indeed satisfied.

Of course, as in the 1D case, in practice the FE formulation is implemented on the element level. Since the volume stiffness matrix $\boldsymbol{K}^a = \mathop{A}_{e=1}^{N_{el}} (\boldsymbol{k}^a)^e$ and the load vector $\boldsymbol{F} = \mathop{A}_{e=1}^{N_{el}} \boldsymbol{f}^e$ are standard, it only remains to consider how the matrix $\boldsymbol{K}^b = \mathop{A}_{e=1}^{N_{el}} (\boldsymbol{k}^b)^e$ should be constructed. (Here N_{el} is the total number of elements and $\mathop{A}_{e=1}^{N_{el}}$ is the FE assembly operator.) For simplicity we assume that the meshes of 2D elements in $\hat{\Omega}_1$ and $\hat{\Omega}_2$ are compatible at the interface B (despite the fact that owing to the jump in u they do not have to be compatible).

One convenient way to construct $\mathbb{K}^b$ is by thinking of the interface B as a collection of *1D interface elements*, sitting on top of the sides of the 2D elements that constitute the meshes in $\hat{\Omega}_1$ and $\hat{\Omega}_2$. Such an interface element occupies the domain B^e and has N_{en} nodes and $2N_{en}$ DOFs, one DOF on each side of the interface. At node a of interface element e, the DOF on the side of the interface adjacent to the region $\hat{\Omega}_j$ is called "DOF j at node a of element e." Then it is easy to infer from (69) and (73) that

$$(\boldsymbol{k}^b)^e = [(k^b)^e_{(ai)(bj)}] \,, \tag{77}$$

$$(k^b)^e_{(ai)(bj)} = \frac{\kappa_L}{2t}\mu_{ij}\int_{B^e}\phi_a\phi_b\,dB \,, \tag{78}$$

$$\mu_{ij} = \begin{cases} 1 & , i = j \\ -1 & , i \neq j \end{cases} \,. \tag{79}$$

Here the indices i and j are the DOF numbers at nodes a and b of element e, and ϕ_a is the element shape function associated with node a.

For example, we consider the simplest case of a *linear* interface element, namely linear shape functions ϕ_a. A simple calculation (note that (78) is reminiscent of a 1D mass matrix) yields the following element stiffness matrix:

$$(\boldsymbol{k}^b)^e = \frac{\kappa_L h^e}{12t}\begin{bmatrix} 2 & -2 & 1 & -1 \\ -2 & 2 & -1 & 1 \\ 1 & -1 & 2 & -2 \\ -1 & 1 & -2 & 2 \end{bmatrix} \,. \tag{80}$$

See Fig. 3 for the identification of the four element DOFs associated with the four row and columns of this matrix.

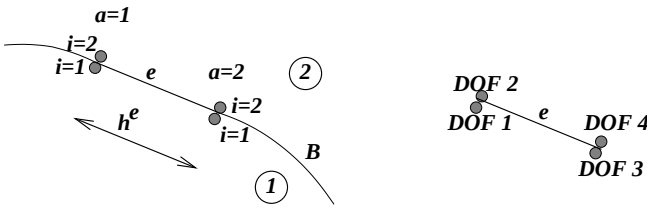

Figure 3 : A 1D interface element.

An alternative convenient way to construct $\mathbb{K}^b$ is to think of the interface element as a *degenerated rectangular element*, as shown in Fig. 4. Geometrically, the thickness

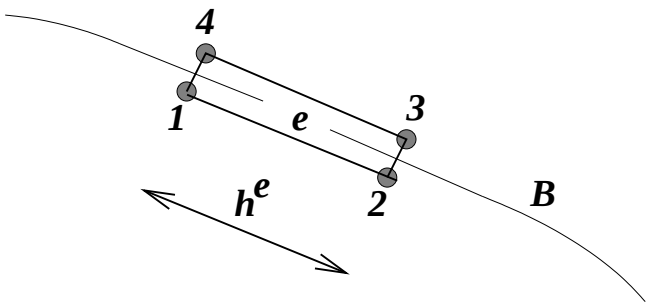

Figure 4 : A degenerated rectangular interface element.

of this element is *zero* (and not the thickness of the layer), namely the nodes 1 and 4 possess the same coordinates, and so do the nodes 2 and 3. The thickness of the layer $2t$ appears only in the factor multiplying the stiffness matrix. The stiffness matrix of the degenerated rectangle is the same as (80) up to changes in the row and column numbers, i.e.,

$$(\boldsymbol{k}^b)^e = \frac{\kappa_L h^e}{12t}\begin{bmatrix} 2 & 1 & -1 & -2 \\ 1 & 2 & -2 & -1 \\ 1 & -2 & 2 & 1 \\ -2 & -1 & 1 & 2 \end{bmatrix} \,. \tag{81}$$

Of course, the two elements just described are essentially identical; they simply provide two different ways of looking at the same implementation. It should be emphasized that although the basic assumption of linear variation in the r direction is common to the degenerated rectangular interface element and to the standard bilinear four-node quadrilateral element, these two elements are totally different. To see this note that the expression for the stiffness matrix (78) of the interface element has no similarity to that of a standard bilinear element.

5.2 Higher-Order Interface Conditions

Now we wish to construct interface conditions of the form (59) and (60), which are more accurate than (61) and (62) in that they take into account the variation of the solution inside the layer in the tangential direction s.

We focus our attention on the vicinity of a certain position along the layer, that we take as $s = 0$ without loss of generality. We consider a slice of the layer of tangential length $2t$ around this position, as shown in Fig. 5. On the edges of the resulting $2t \times 2t$ square we identify the 8 points u_j, ${}^*u_j$, u^*_j, ${}^*\overline{u}$ and $\overline{u}^*$, and the central point $\overline{u}$.

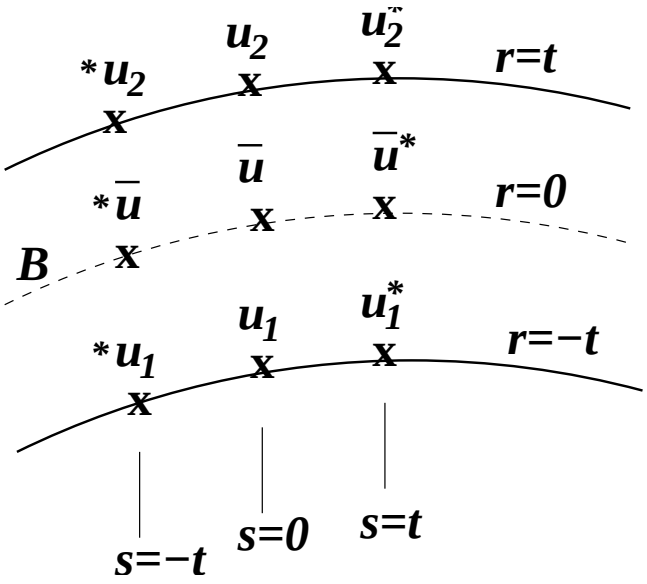

Figure 5 : Setup for constructing the higher-order interface conditions in 2D.

We assume a *parabolic* variation of the solution in the tangential direction inside the slice. Thus, on the two edges $r=-t$ and $r=t$ we have

$$u(-t,s) = C^- + D^- s + E^- s^2 \ ,$$
$$u(+t,s) = C^+ + D^+ s + E^+ s^2 \ . \tag{82}$$

From this we easily deduce:

$$C^\pm = u(\pm t,0) \quad , \quad D^\pm = u_{,s}(\pm t,0) \quad ,$$
$$E^\pm = \frac{1}{2} u_{,ss}(\pm t,0) \ . \tag{83}$$

From (82) and (83) we get (see Fig. 5)

$$^*u_1 = u(-t,-t) = u_1 - t u_{1,s} + \frac{t^2}{2} u_{1,ss} \ , \tag{84}$$

$$u_1^* = u(-t,t) = u_1 + t u_{1,s} + \frac{t^2}{2} u_{1,ss} \ , \tag{85}$$

$$^*u_2 = u(t,-t) = u_2 - t u_{2,s} + \frac{t^2}{2} u_{2,ss} \ , \tag{86}$$

$$u_2^* = u(t,t) = u_2 + t u_{2,s} + \frac{t^2}{2} u_{2,ss} \ . \tag{87}$$

Assuming a linear variation in r in the tangential positions $s=\pm t$, we can calculate $^*\overline{u}$ and $\overline{u}^*$ as the averages of the quantities given above, i.e.,

$$^*\overline{u} = \frac{1}{2}(^*u_1 + {}^*u_2)$$
$$= \frac{1}{2}\left(u_1 + u_2 - t(u_{1,s} + u_{2,s}) + \frac{t^2}{2}(u_{1,ss} + u_{2,ss}) \right) \ , \tag{88}$$

$$\overline{u}^* = \frac{1}{2}(u_1^* + u_2^*)$$
$$= \frac{1}{2}\left(u_1 + u_2 + t(u_{1,s} + u_{2,s}) + \frac{t^2}{2}(u_{1,ss} + u_{2,ss}) \right) \ . \tag{89}$$

Now we wish to estimate the value of $\overline{u}$, at the central point. Of course we may take $\overline{u} = (1/2)(u_1+u_2)$, but this approximation will not make use of the variation of u in s and will lead us back to the interface condition obtained in Section 5.1. A better approximation is based on the average of the four values at the points neighboring to the central point, i.e.,

$$\overline{u} = \frac{1}{4}(u_1 + u_2 + {}^*\overline{u} + \overline{u}^*) \ . \tag{90}$$

The weights of the four values in this formula are the same since the four points are equally distanced from the central point. Substituting (88) and (89) in (90) results in

$$\overline{u} = \frac{1}{8}(4u_1 + 4u_2 + t^2 u_{1,ss} + t^2 u_{2,ss}) \ . \tag{91}$$

Now, based on the values u_1, $\overline{u}$ and u_2 we can estimate the normal derivatives $u_{,n}(-t,0)$ and $u_{,n}(t,0)$ by assuming a piecewise-linear variation of u in the thickness direction:

$$u_{,n}(-t,0) = \frac{\overline{u} - u_1}{t}$$
$$= \frac{1}{8t}(-4u_1 + 4u_2 + t^2 u_{1,ss} + t^2 u_{2,ss}) \ , \tag{92}$$

$$u_{,n}(t,0) = \frac{u_2 - \overline{u}}{t}$$
$$= \frac{1}{8t}(-4u_1 + 4u_2 - t^2 u_{1,ss} - t^2 u_{2,ss}) \ . \tag{93}$$

From this and from the original continuity conditions (cf. (47) and (48)) we get the boundary conditions

$$\kappa_1 u_{,n}^- = \frac{\kappa_L}{8t}(-4u^- + 4u^+ + t^2 u_{,ss}^- + t^2 u_{,ss}^+) \ , \tag{94}$$

$$\kappa_2 u_{,n}^+ = \frac{\kappa_L}{8t}(-4u^- + 4u^+ - t^2 u_{,ss}^- - t^2 u_{,ss}^+) \ . \tag{95}$$

These are the desired interface conditions, which have exactly the form (59) and (60).

These interface conditions can be incorporated in the weak form of the problem, and lead (after integration by parts along B) to a symmetric C^0 FE formulation. However, we note that for typical layers the last two terms on the right side of (94) and (95) are negligible compared to the first two terms, since they are of order t^2. If we neglect them we get the simpler interface conditions

$$\kappa_1 u^-_{,n} \simeq \kappa_2 u^+_{,n} \simeq \frac{\kappa_L}{2t}[u] \ , \tag{96}$$

which are in fact (61) and (62). We thus conclude that usually the higher-order terms in the interface conditions, which turn out to be $O(t^2)$, do not increase the accuracy significantly.

6 Extensions

6.1 Three Dimensions

In 3D the layer occupies a volume, and is replaced by an interface which is a surface. The extension of the interface conditions (61) and (62) and the FE formulation (68)–(74) to the 3D case is immediate; they essentially remain the same. The higher-order conditions (94) and (95) can also easily be extended by adding the appropriate terms in the second tangential direction. They are obtained by considering a $2t \times 2t \times 2t$ cube analogous to the square in Fig. 5. However, as in 2D, the higher-order terms are $O(t^2)$ and are thus typically negligible.

6.2 External Coating

If the layer is *external*, as in the case of a structure which is externally coated, then the problem involves only *two* phases: the layer and the medium it rests upon. In this case the "interface" B is an external boundary. Still it is necessary to consider two sets of DOFs on the interface, i.e., $u_1 = u^-$ which is inward and $u_2 = u^+$ which is outward, as in Fig. 3.

For example, we consider a simply-connected 2D domain Ω occupied by material with conductivity κ_1 encapsulated by thin coating with conductivity κ_L. The external boundary of the coating is Γ. We consider the differential equation (45) in Ω, and the flux-transfer boundary condition

$$\kappa_L u_{,n} = \alpha(u_\infty - u) \quad \text{on} \quad \Gamma \ . \tag{97}$$

Here α and u_∞ are the given coefficient of flux transfer and the environment field, respectively. We replace the layer by a boundary B which coincides with Γ. (Whether B passes in the middle of the layer or lies on its outer boundary Γ is not important as long as the layer is thin.) The approximate interface conditions are then

$$\kappa_1 u^-_{,n} = \frac{\kappa_L}{2t}[u] \ , \tag{98}$$

$$\alpha(u_\infty - u^+) = \frac{\kappa_L}{2t}[u] \ . \tag{99}$$

These conditions can easily be incorporated in a FE formulation. The weak equation is (67), with the bilinear forms

$$a(w,u) = a_1(w,u) \ , \tag{100}$$

$$b(w,u) = \frac{\kappa_L}{2t}\int_B [w][u]\,dB + \int_B w^+ \alpha u^+ \,dB \ , \tag{101}$$

$$(w,f) = (w,f)_1 + \int_B w^+ \alpha u_\infty \,dB \ . \tag{102}$$

By comparing this to (68)–(74), we see that the terms pertaining to Ω_2 have been dropped here, and instead some new terms appear that are associated with the flux-transfer condition (97). The FE formulation remains symmetric and positive definite.

6.3 Elasticity

The analogous treatment of layers in linear elastic media is technically more complicated than the scalar case considered so far. We consider a linear elastic solid composed of three phases, $k = 1, L, 2$, as shown in Fig. 1. The given continuity conditions on each side of the layer are the continuity of displacements and tractions:

$$\begin{aligned} u_i^{(1)} &= u_i^{(L)} \quad , \quad T_i^{(1)} = T_i^{(L)} \ , \\ u_i^{(2)} &= u_i^{(L)} \quad , \quad T_i^{(2)} = T_i^{(L)} \ . \end{aligned} \tag{103}$$

We assume each phase to be isotropic. In particular, inside the layer, in the directions normal and tangential to the layer, the following stress-strain relations hold:

$$\sigma_{rr}^{(L)} = (\lambda^{(L)} + 2G^{(L)})\varepsilon_{rr}^{(L)} + \lambda^{(L)}\varepsilon_{ss}^{(L)} \ , \tag{104}$$

$$\sigma_{ss}^{(L)} = (\lambda^{(L)} + 2G^{(L)})\varepsilon_{ss}^{(L)} + \lambda^{(L)}\varepsilon_{rr}^{(L)} \ , \tag{105}$$

$$\sigma_{rs}^{(L)} = 2G^{(L)}\varepsilon_{rs}^{(L)} \ . \tag{106}$$

Here $\lambda^{(L)}$ and $G^{(L)}$ are the Lamé constants of the layer material. From the relations between tractions T_i and stresses σ_{ij}, and from the relations between strains ε_{ij} and displacements u_i, i.e.,

$$T_i = \sigma_{ij} n_j \qquad , \qquad \varepsilon_{ij} = \frac{1}{2}(u_{i,j} + u_{j,i}) \; , \tag{107}$$

we can write (104) and (106) as

$$T_r^{(L)} = (\lambda^{(L)} + 2G^{(L)}) u_{r,r}^{(L)} + \lambda^{(L)} u_{s,s}^{(L)} \; , \tag{108}$$

$$T_s^{(L)} = G^{(L)} (u_{s,r}^{(L)} + u_{r,s}^{(L)}) \; . \tag{109}$$

In order to be able to replace the layer with an interface, we need to express the continuity conditions (103) in terms of $u_i^{(1)}$ and $u_i^{(2)}$ only. From (108) and (109) we get, by assuming a linear variation of the displacement in the thickness direction of the layer,

$$T_r^{(1)} = (\lambda^{(L)} + 2G^{(L)}) \frac{u_r^{(2)} - u_r^{(1)}}{2t} + \lambda^{(L)} u_{s,s}^{(1)} \; , \tag{110}$$

$$T_r^{(2)} = (\lambda^{(L)} + 2G^{(L)}) \frac{u_r^{(2)} - u_r^{(1)}}{2t} + \lambda^{(L)} u_{s,s}^{(2)} \; , \tag{111}$$

$$T_s^{(1)} = G^{(L)} \frac{u_s^{(2)} - u_s^{(1)}}{2t} + G^{(L)} u_{r,s}^{(1)} \; , \tag{112}$$

$$T_s^{(2)} = G^{(L)} \frac{u_s^{(2)} - u_s^{(1)}}{2t} + G^{(L)} u_{r,s}^{(2)} \; . \tag{113}$$

In deriving these relations we have used the original continuity conditions (103) as well as the fact that if a quantity is continuous across an interface so is its tangential derivative. Now the layer may be replaced by the interface B, and (110)–(113) become the interface conditions

$$T_r^- = \frac{\lambda^{(L)} + 2G^{(L)}}{2t} [u_r] + \lambda^{(L)} u_{s,s}^- \; , \tag{114}$$

$$T_r^+ = \frac{\lambda^{(L)} + 2G^{(L)}}{2t} [u_r] + \lambda^{(L)} u_{s,s}^+ \; , \tag{115}$$

$$T_s^- = \frac{G^{(L)}}{2t} [u_s] + G^{(L)} u_{r,s}^- \; , \tag{116}$$

$$T_s^+ = \frac{G^{(L)}}{2t} [u_s] + G^{(L)} u_{r,s}^+ \; . \tag{117}$$

These interface conditions are now incorporated in a FE formulation. The weak form of the problem is governed by the equation

$$a(w,u) + b(w,u) = z(w) \; . \tag{118}$$

The bilinear form $a(w,u)$ and the linear form $z(w)$ are the standard ones while $b(w,u)$ originates from the interface conditions. A straight forward derivation using (114)–(117) leads to

$$\begin{aligned} b(w,u) &= \int_B \left\{ \frac{\lambda^{(L)} + 2G^{(L)}}{2t} [w_r][u_r] + \frac{G^{(L)}}{2t} [w_s][u_s] \right. \\ &\left. - \lambda^{(L)} (w_r^- u_{s,s}^- + w_r^+ u_{s,s}^+) - G^{(L)} (w_s^- u_{r,s}^- + w_s^+ u_{r,s}^+) \right\} dB \; . \end{aligned} \tag{119}$$

Note that the terms on the second line of (119) make this bilinear form *non-symmetric*.

One way to render the formulation symmetric is to simply ignore the non-symmetric terms in (119). This amounts to neglecting the s-derivative terms in the interface conditions (114)–(117) compared to the other terms, i.e.,

$$T_r^- = T_r^+ = \frac{\lambda^{(L)} + 2G^{(L)}}{2t} [u_r] \; , \tag{120}$$

$$T_s^- = T_s^+ = \frac{G^{(L)}}{2t} [u_s] \; . \tag{121}$$

Neglecting the s-derivative terms in (114)–(117) can be justified by using arguments similar to those made is Section 5.1.

Another option for rendering the bilinear form $b(\cdot,\cdot)$ symmetric is to scale the weighting functions w_r and w_s differently, namely to define

$$W_r = \lambda_L w_r \qquad , \qquad W_s = -G_L w_s \; . \tag{122}$$

With the new weighting functions W_r and W_s, and after applying integration by parts to (119), the formulation becomes symmetric. However, the disadvantage of this procedure is that the standard terms (and element matrices) are also affected by this scaling. Thus, using (122) means that one has to modify the entire FE formulation, not just to add an interface term to it.

7 Numerical Experiments

In this section we test the proposed methodology, and in particular the FE formulation (68)–(74). To this end we consider the relatively simple two-dimensional setup described in Fig. 6. Linear heat conduction may be thought

of as the underlying physical model, although any other phenomenon governed by Laplace's equation would be appropriate as well. A layer of length a and thickness $2t$, made of a weakly-conducting material, is situated between two rectangular blocks of well-conducting material. The origin of the system of coordinates lies on the left edge in the middle of the layer such that the domain Ω_L which the layer occupies is given by $0 \le x \le a$, $-t \le y \le t$. The widths of the two rectangular conducting blocks, occupying the domains Ω_1 and Ω_2, are b_1 and b_2, as indicated in the figure. The entire domain is denoted Ω and its exterior boundary is denoted Γ.

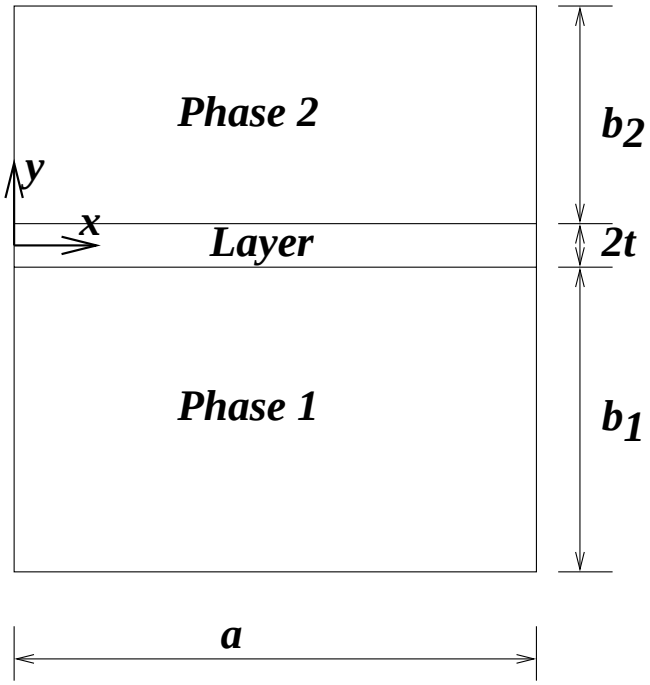

Figure 6 : Example model of a thin weakly-conducting layer between two phases of conducting material.

The conductivities of the three phases are denoted κ_1, κ_L and κ_2, and are taken to be constant. In each of the three open domains Laplace's equation holds:

$$\nabla^2 u \equiv \frac{\partial^2 u}{\partial x^2} + \frac{\partial^2 u}{\partial y^2} = 0 \quad \text{in} \quad \Omega_1,\ \Omega_L\ ,\Omega_2\ . \tag{123}$$

We consider two specific solutions, piecewise linear and piecewise parabolic, which satisfy (123). In each case we design the boundary conditions on Γ to satisfy this solution. Thus, the exact solution is known by construction, which is useful for calculating the error generated by the computational scheme. Neumann boundary conditions are calculated from the exact solution and are imposed along Γ, except at the lower left corner ($x = 0$, $y = -(b_1 + t)$) where a Dirichlet condition is imposed to make the solution unique. In addition to (123) and the exterior boundary conditions, the original problem includes continuity conditions on the two faces of the layer (see (47) and (48)), i.e.,

$$\begin{aligned} &u_1(x,-t) = u_L(x,-t)\ , \\ &u_L(x,t) = u_2(x,t)\ , \end{aligned} \tag{124}$$

$$\begin{aligned} &\kappa_1 \frac{\partial u_1}{\partial y}(x,-t) = \kappa_L \frac{\partial u_L}{\partial y}(x,-t)\ , \\ &\kappa_L \frac{\partial u_L}{\partial y}(x,t) = \kappa_2 \frac{\partial u_2}{\partial y}(x,t)\ . \end{aligned} \tag{125}$$

We take $\kappa_1 = \kappa_2 = 1$, and leave $\kappa_L < 1$ a free parameter. The case $\kappa_L > 1$ is less interesting since in the case of a well-conducting layer one may often ignore the layer without generating significant errors. The opposite case, of an ill-conducting layer, is both physically more interesting and computationally more difficult.

Throughout this experiment we use meshes of rectangular FEs with bilinear shape functions. We set $a = 10$ and $b_1 = b_2 = 5$, and we leave the half-thickness of the layer t to be a second free parameter. In each of phases 1 and 2 we use 20 elements in the x direction and 15 elements in the y direction. As to the treatment of the layer we consider three schemes:

- **S1:** *Fully modeling the layer by standard FEs.* We use five bilinear elements in the thickness direction (namely an overall number of 100 elements) to represent the layer.
- **S2:** *Using the new interface scheme* proposed in the paper, based on the FE formulation (68)–(74).
- **S3:** *Ignoring the layer.* There are a number of ways that this can be done. We do this by thinking of the layer as belonging to phase 1 in all respects. Thus, in this model we only have two phases with two conductivities: κ_1 and κ_2.

Our first experiment concerns a problem whose solution is a piecewise linear function. This serves as a sort of a

Table 1 : Summarizes the errors generated by schemes S1, S2 and S3 for various values of the layer thickness $2t$ and the layer conductivity κ_L.

$2t$	κ_L	'Layer' model **S1**		'Interface' model **S2**		'Ignore' model **S3**	
		E_Ω	E_B	E_Ω	E_B	E_Ω	E_B
0.5	0.1	0.12E-04	0.11E-04	0.54E-02	0.87E-02	0.44E-01	0.64E-01
0.5	0.01	0.12E-04	0.11E-04	0.55E-03	0.87E-03	0.44E-01	0.64E-01
0.5	0.001	0.69E-07	0.37E-10	0.54E-04	0.87E-04	0.48E-01	0.71E-01
0.5	0.0001	0.61E-05	0.54E-05	0.53E-05	0.83E-05	0.49E-01	0.71E-0
0.05	0.1	0.91E-05	0.81E-05	0.54E-03	0.86E-03	0.48E-02	0.76E-02
0.05	0.01	0.30E-05	0.27E-05	0.56E-04	0.88E-04	0.53E-02	0.83E-02
0.05	0.001	0.30E-05	0.27E-05	0.44E-05	0.79E-05	0.53E-02	0.84E-02
0.05	0.0001	0.42E-04	0.37E-04	0.42E-04	0.38E-04	0.53E-02	0.84E-02
0.005	0.1	0.11E-04	0.10E-04	0.48E-04	0.83E-04	0.49E-03	0.78E-03
0.005	0.01	0.14E-04	0.12E-04	0.17E-04	0.17E-04	0.53E-03	0.85E-03
0.005	0.001	0.81E-04	0.72E-04	0.81E-04	0.72E-04	0.54E-03	0.86E-03
0.005	0.0001	0.86E-03	0.76E-03	0.86E-03	0.76E-03	0.54E-03	0.86E-03

"patch test" to validate the new interface scheme. The exact solution is

$$u_1 = \frac{\kappa_L}{\kappa_1}(y+t) - t \ , \tag{126}$$

$$u_2 = \frac{\kappa_L}{\kappa_2}(y-t) + t \ , \tag{127}$$

$$u_L = y \ . \tag{128}$$

It is easy to check that this solution satisfies (123)–(125). We have solved the problem with various values of t and $0 < \kappa_L < 1$. In all cases both schemes S1 and S2 yielded the exact solution to within machine precision. The fact that S1 generates zero error is obvious; it follows from the ability of the shape functions to exactly represent global piecewise-linear functions. (This can be regarded as a consequence of the Best Approximation property; see Hughes [Hughes (1987)].) The fact that our new interface scheme S2 also generates zero error for such problems shows that this scheme indirectly possesses the piecewise-linear representation property as well. Needless to say, S3 (which ignores the layer) generates nonzero errors.

Next, we consider a problem whose solution is piecewise-parabolic. The solution is given by

$$u_1 = x^2 + B_1(y+t) - y^2 \ , \tag{129}$$

$$u_2 = x^2 - B_2(y-t) - y^2 \ , \tag{130}$$

$$u_L = x^2 - y^2 \ , \tag{131}$$

$$B_1 = 2t\left(\frac{\kappa_L}{\kappa_1} - 1\right) \qquad , \qquad B_2 = 2t\left(\frac{\kappa_L}{\kappa_2} - 1\right) \ . \tag{132}$$

Again, it is easy to check that this solution satisfies (123)–(125). Obviously, for such a problem none of the schemes S1, S2 or S3 would yield the exact solution as long as bilinear shape functions are used.

To measure the numerical error, we define two global error measures:

$$E_\Omega^2 \equiv \frac{\sum_{A\in\eta_\Omega}(u_A - u_A^h)^2}{\sum_{A\in\eta_\Omega} u_A^2} \ , \tag{133}$$

$$E_B^2 \equiv \frac{\sum_{A\in\eta_B}(u_A - u_A^h)^2}{\sum_{A\in\eta_B} u_A^2} \ . \tag{134}$$

Here u is the exact solution, u^h is the FE solution, the index A stands for a node number, η_Ω is the set of all the mesh nodes and η_B is the set of all the nodes on the boundary B. Thus, E_Ω and E_B are, respectively, the relative discrete l_2 (Euclidian) norm of the error in the entire mesh and on B.

The following can be concluded from Table 1:

- In general, the full layer model S1 generates the least error (maximum of 0.086% in the cases reported in the table), and the model S3 ignoring the layer yields the largest error (maximum of 7.1%).

The new interface model S2 generates an intermediate level of errors (maximum of 0.87%). This result is expected and demonstrates that the goal associated with the interface scheme S2 is achieved.

- The S2 and S3 errors are almost linear with the layer thickness $2t$. The increase of the error with $2t$ is also expected: for a thicker layer the error associated with the interface model or with the model which ignores the layer becomes larger.

- The S3 error hardly depends on the layer conductivity κ_L, whereas the S2 error is almost linear with κ_L, except for very small layer thicknesses. To understand the decrease of the S2 error with the decrease of κ_L, note that in the limit $\kappa_L \to 0$ the conditions (125) become

$$\kappa_1 \frac{\partial u_1}{\partial y}(x,-t) = 0 \qquad , \qquad \kappa_2 \frac{\partial u_2}{\partial y}(x,t) = 0 \, , \quad (135)$$

  which are the same as the approximate interface conditions (61) and (62) in the same limit.

- For very small layer thickness $2t$, the S2 error becomes close to the S1 error, namely recovers the exact solution up to the unavoidable FE approximation errors. On the other hand, the S3 error remain an order of magnitude larger, except for very small values of κ_L.

- When both $2t$ and κ_L are very small, the problem becomes "hard": the errors in the S1 and S2 schemes increase and approach the S3 error. This is the regime where round-off errors become significant and the solution starts to lose its stability.

We remark that the linear behavior of the errors with $2t$ and κ_L is related to the approximation error of a parabolic function by a linear function, and is probably problem dependent.

For the specific case $2t = 0.5$ and $\kappa_L = 0.1$, Fig. 7 compares the exact solution to the S2 and S3 solutions. (The S1 solution practically coincides with the exact solution.) It is clear that whereas the S2 solution ('interface' model) remains very close to the exact solution (Fig. 7(a)), the S3 solution ('ignore' model) is significantly off (Fig. 7(b)). Note especially the spurious divergence of the contour lines on the left side of the figure as well as the 'wiggle' on the right side.

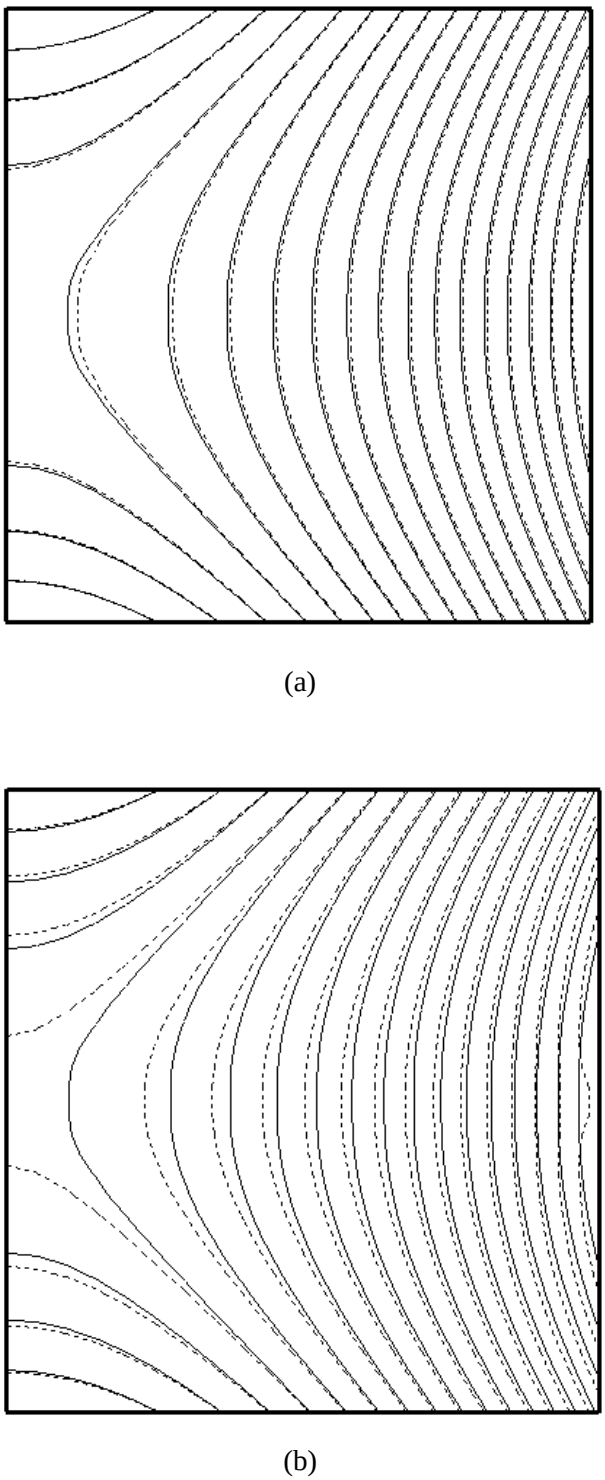

(a)

(b)

Figure 7 : Contour lines of the solution for the case $2t = 0.5$, $\kappa_L = 0.1$. The solid lines in each figure are those of the exact solution. The dashed lines correspond to the (a) S2 solution ('interface' model) and (b) S3 solution ('ignore' model).

To further examine the layer representation error we consider another error measure, namely the relative maximum-norm error defined by

$$e_{\max} \equiv \frac{\max_{A\in\eta_\Omega} |u_A - u_A^h|}{\max_{A\in\eta_\Omega} |u_A|} \ . \tag{136}$$

Fig. 8 shows, on a log-log scale, the error $e_{\max}$ generated by the three schemes as a function of the layer thickness $2t$, with the fixed layer conductivity value $\kappa_L = 0.1$. The linearity of the S2 and S3 errors with the layer thickness is clear. For this value of κ_L the S2 scheme is more accurate by an order of magnitude than the S3 scheme for the entire range of thickness values.

Fig. 9 shows the same error as a function of the layer conductivity κ_L, with the fixed layer thickness value $2t = 0.5$. For this value of thickness and for sufficiently small κ_L the S2 error is much smaller than the S3 error. However, the S3 error remains constant while the S2 error increases with κ_L as the figure shows. For $\kappa_L \simeq \kappa_1 = 1$ the S3 solution is more accurate, provided that the layer is sufficiently thick. However, this is not a particularly interesting case for two reasons: (a) thick layers indeed should not be treated by the interface approximation proposed here or any other method of approximating the layer; (b) when $\kappa_L \simeq \kappa_1 = 1$ the layer can indeed be ignored without major consequences.

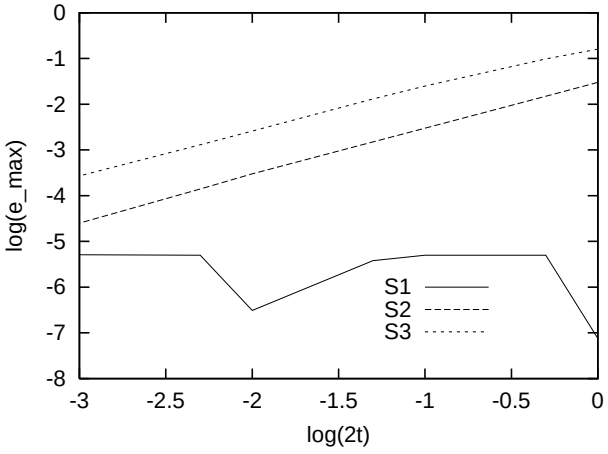

Figure 8 : The relative maximum error generated by the three schemes as a function of the layer thickness $2t$, for $\kappa_L = 0.1$.

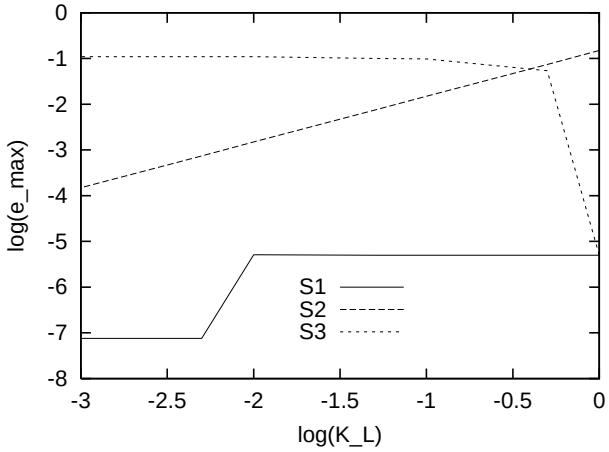

Figure 9 : The relative maximum error generated by the three schemes as a function of the layer conductivity κ_L, for $2t = 0.5$.

8 Concluding Remarks

We have proposed a simple technique to model thin layers within the finite element methodology. The layer is modelled as an interface and appropriate jump conditions are imposed on it. This method constitutes a prudent compromise between the two traditional ways of handling a thin layer: fully modeling it using standard finite elements or simply ignoring it. The proposed method is less expensive computationally than the former and much more accurate than the latter.

The method was presented in various configurations and variants. Its good performance was demonstrated here via numerical experiments in the two dimensional scalar case, like that of heat conduction. The example chosen here is very simple in its geometry and governing equations, but succeeds to illuminate the main properties of the proposed method. Further development of the method should include implementation and thorough investigation in more complicated situations, such as the elastic case and the three-dimensional case. In addition, theoretical error analysis is needed to support the findings reported in the previous section (and in particular to explain the linear dependencies seen in Table 1) and to predict the convergence rate in general. We hope to report on these matters in a future publication.

Acknowledgement: This work was supported in part by the Technion's R.&M. Rosenthal Aerospace Eng. Re-

search Fund and by the Technion's Fund for the Promotion of Research.

References

Achenbach, J. D.; Zhu, H. (1989): Effect of Interfacial Zone on Mechanical Behaviour and Failure of Fibre-Reinforced Composites, *J. Mech. Phys. Solids*, 37, 381–393.

Achenbach, J. D.; Zhu, H. (1990): Effect of Interphases on Micro and Macromechanical Behavior of Hexagonal-Array Fiber Composites, *ASME J. of Appl. Mech.*, 57, 956–963.

Barbone, P.; Givoli, D.; Patlashenko, I. (2003): Optimal Modal Reduction of Vibrating Substructures, *Int. J. Numer. Meth. Engng.*, 57, 341–369.

Body, C.; Reyne, G.; Meunier, G. (1997): Nonlinear Finite Element Modelling of Magneto-Mechanical Phenomenon in Giant Magnetostrictive Thin Films, *IEEE Trans. Magnetics*, 33, 1620–1623.

Boutry, M.; Bosseboeuf, A.; Grandchamp, J. P.; Coffignal, G. (1997): Finite-Element Method Analysis of Freestanding Microrings for Thin-Film Tensile Strain Measurements, *J. Micromechanics and Microengineering*, 7, 280–284.

Cai, X.; Bangert, H. (1996): Finite-Element Analysis of the Interface Influence on Hardness Measurements of Thin Films, *Surface & Coatings Tech.*, 81, 240–255.

Chen, X. L.; Liu, Y. J. (2001): Thermal Stress Analysis of Multi-Layer Thin Films and Coatings by an Advanced Boundary Element Method, *CMES: Computer Modeling in Engineering & Sciences*, 2, 337–349.

Genna, F.; Paganelli, C.; Salgarello, S.; Sapelli, P. (2003): 3-D Numerical Analysis of the Stress State Caused by Short-Term Loading of a Fixed Dental Implant Containing a "PDL-Like" Nonlinear Elastic Internal Layer, *CMES: Computer Modeling in Engineering & Sciences*, 4, 405–420.

Givoli, D. (1999a): Exact Representations on Artificial Interfaces and Applications in Mechanics, *Appl. Mech. Rev.*, 52, 333–349.

Givoli, D. (1999b): Recent Advances in the DtN Finite Element Method for Unbounded Domains, *Archives of Comput. Meth. in Engng.*, 6, 71–116.

Givoli, D.; Patlashenko, I. (2002): An Optimal High-Order Non-Reflecting Finite Element Scheme for Wave Scattering Problems, *Int. J. Numer. Meth. Engng.*, 53, 2389–2411.

Givoli, D.; Rivkin, L.; Keller, J. B. (1992): A Finite Element Method for Domains With Corners, *Int. J. Numer. Meth. Engng.*, 35, 1329–1345.

Hashin, Z. (2001): Thin Interphase/Imperfect Interface in Conduction, *J. Appl. Phys.*, 89, 2261–2267.

Hashin, Z. (2002): Thin Interphase/Imperfect Interface in Elasticity With Application to Coated Fiber Composites, *J. Mech. Phys. Solids*, 50, 2509–2537.

Hoppe, R. H. W.; Nash, E. M. (2002): A Combined Spectral Element/Finite Element Approach to the Numerical Solution of a Nonlinear Evolution Equation Describing Amorphous Surface Growth of Thin Films, *J. Numer. Math.*, 10, 127–136.

Hughes, T. J. R. (1987): *The Finite Element Method*, Prentice-Hall, New Jersey.

Keller, J. B.; Givoli, D. (1989): Exact Non-Reflecting Boundary Conditions, *J. Comput. Phys.*, 82, 172–192.

Masters, C. B.; Salamon, N. J. (1994): Geometrically Nonlinear Stress-Deflection Relations for Thin Film/Substrate Systems With a Finite Element Comparison, *ASME J. of Appl. Mech.*, 61, 872–878.

Sham, T. L.; Tichy, J. (1997): Scheme for Hybrid Molecular Dynamics/Finite Element Analysis of Thin Film Lubrication, *Wear*, 207, 100–106.

Subramaniam, A.; Ramakrishnan, N. (2003): Analysis of Thin Film Growth Using Finite Element Method, *Surface and Coatings Tech.*, 167, 249–254.

Suess, D.; Tsiantos, V.; Schrefl, T.; Scholz, W.; Fidler, J. (2002): Nucleation in Polycrystalline Thin Films Using a Preconditioned Finite Element Method, *J. Applied Phys.*, 91, 7977–7987.

Sung, J.; Choi, H. G.; Yoo, J. Y. (1999): Finite Element Simulation of Thin Liquid Film Flow and Heat Transfer Including a Hydraulic Jump, *Int. J. Numer. Meth. Engng.*, 46, 83–101.

Yue, Z. F.; Eggeler, G.; Stockhert, B. (2001): A Creep Finite Element Analysis of Indentation Creep Testing in Two Phase Microstructures, *Comput. Mater. Sci.*, 21, 37–56.

Zhang, Y. W.; Bower, A. F.; Xia, L.; Shih, C. F. (1999): Three Dimensional Finite Element Analysis of the Evolution of Voids and Thin Films by Strain and Electromigration Induced Surface Diffusion, *J. Mech. Phys. Solids*,

47, 173–199.

Zhang, J. M.; Yao, Z. H. (2002): Analysis of 2-D Thin Structures by the Meshless Regular Hybrid Boundary Node Method, *Acta Mech. Solida Sin.*, 15, 36–44.